Analysis of lake ice dynamics and morphology on Lake El'gygytgyn, NE Siberia, using synthetic aperture radar (SAR) and Landsat

Matt Nolan,[1] Glen Liston,[2] Peter Prokein,[1] Julie Brigham-Grette,[3] Virgil L. Sharpton,[4] and Rachel Huntzinger[1]

Received 7 June 2001; revised 17 January 2002; accepted 17 May 2002; published 27 November 2002.

[1] A time series of more than 450 combined ERS-2, Radarsat-1, and Landsat-7 scenes acquired between 1998 and 2001 was analyzed to develop a fairly complete picture of lake ice dynamics on Lake El'gygytgyn, NE Siberia (67.5°N, 172°E). This 14-km^3 lake partially fills a meteorite impact crater formed 3.6 million years ago and is home to a paleoenvironmental coring project. The duration of lake ice cover and the onset of lake ice breakup are important both to interpretations of the archived sediment core record and to future drilling projects that will use the ice as a stable platform. Ice formation, snowmelt, and ice breakup likely occur in late October, mid-May, and early July, respectively. These data were used to validate a one-dimensional energy-balance lake ice model, which can now be used to hindcast paleoclimate based on core proxy information. Synthetic aperture radar (SAR) backscatter from the lake ice also revealed unusual spatial variations in bubble content, which were found to indicate the level of biological productivity in the sediments directly beneath the ice, with the highest productivity located in the shallowest (0–10 m) as well as the deepest (170–175 m) regions of the lake. Seismic data indicates that the backscatter anomaly above the deepest water is collocated with the central peak of the impact crater, 500 m below the surface. Several hypotheses are presented to explain this anomaly. Regardless of cause, the fact that large spatial variations in biological productivity exist in the lake has important implications for selecting the locations of future sediment cores. *INDEX TERMS:* 1640 Global Change: Remote sensing; 1845 Hydrology: Limnology; 1630 Global Change: Impact phenomena; 1863 Hydrology: Snow and ice (1827); 1878 Hydrology: Water/energy interactions; 1615 Global Change: Biogeochemical processes (4805); *KEYWORDS:* lake ice, energy balance, lake modeling, Chukotka, Russia, climate

Citation: Nolan, M., G. Liston, P. Prokein, J. Brigham-Grette, V. L. Sharpton, and R. Huntzinger, Analysis of lake ice dynamics and morphology on Lake El'gygytgyn, NE Siberia, using synthetic aperture radar (SAR) and Landsat, *J. Geophys. Res.*, *107*, 8162, doi:10.1029/2001JD000934, 2002. [printed *108*(D2), 2003]

1. Introduction

1.1. Background

[2] El'gygytgyn Crater (pronounced el-jē-git'-gin) was formed by a meteorite impact 3.6 million years ago [*Layer*, 2000], at 67.5°N and 172°E (Figure 1), and the lake that formed inside it has since become an excellent paleoenvinronmental archive site. At the time of impact, most of the Arctic was forested all the way to the Arctic Ocean, and a million years passed before the first glaciation of the Northern Hemisphere began [*Brigham-Grette and Carter*, 1992]. The lake is currently about 12 km in diameter and sits inside a crater roughly 18 km in diameter. The maximum lake depth is about 175 m, with more than 350 m of sediments deposited since the impact [*Niessen et al.*, 2000]. This large oligotrophic lake has a volume of 14.1 km^3 and a surface area of 117 km^2, with approximately 50 inlet streams draining the 293 km^2 crater area (Nolan, unpublished data). It is located in a remote area of Chukotka that is rarely visited by humans. The crater is the best preserved on Earth for its size [*Dence*, 1972; *Dietz and McHone*, 1976], and the lake is only one of a handful formed inside of craters identified as impact craters [*Lehman et al.*, 1995]. The lake has likely never gone dry since its formation (M. Nolan, unpublished data, 2000) and the area has never been glaciated [*Glushkova*, 1993], indicating that sediments here are continuous and undisturbed. In winter of 1998 we recovered a sediment core containing a 300,000 year climate-record from Lake El'gygytgyn (Lake E); this is the oldest terrestrial sediment core yet recovered from the Arctic. Core interpretations have already yielded important controls on the state of the hydrological cycle, the energy balance, the

[1]Water and Environmental Research Center, Institute of Northern Engineering, University of Alaska Fairbanks, Fairbanks, Alaska, USA.
[2]Department of Atmospheric Sciences, Colorado State University, Colorado, USA.
[3]Department of Geosciences, University of Massachusetts Amherst, Amherst, Massachusetts, USA.
[4]Geophysical Institute, University of Alaska Fairbanks, Fairbanks, Alaska, USA.

0148-0227/02/2001JD000934$09.00

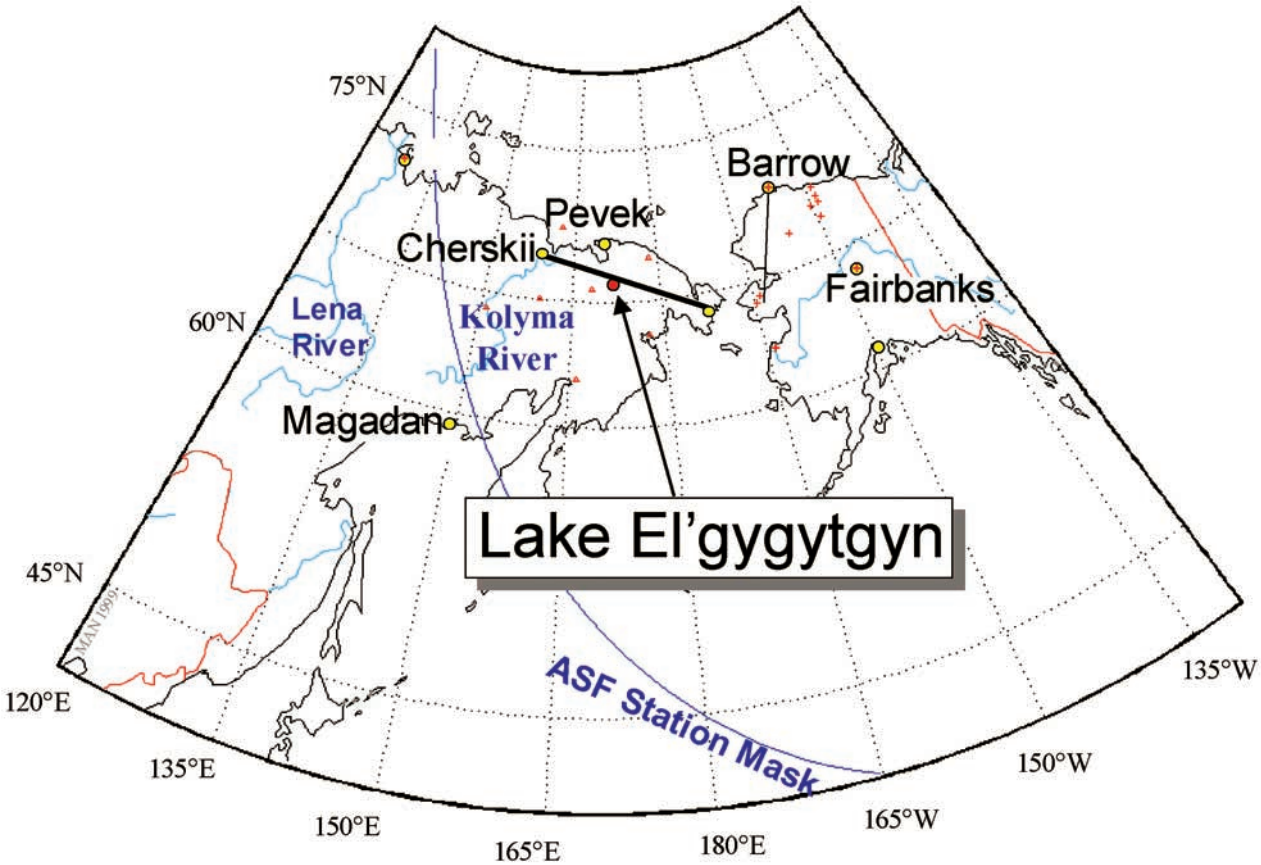

Figure 1. Location map for Lake El'gygytgyn and the Northern Far East transect. Lake E sits near the center of a cooling anomaly [*Chapman and Walsh*, 1993]; since that study several of the Russian met stations (red dots) used have stopped recording. Lake E is also the midpoint of the Northern Far East transect of NSF climate, vegetation, and flux studies in Russia (thick line), from Cherskii to Lavrentia. All sites within this transect are located within the receiving mask of the Alaska SAR Facility. The results of this transect will be compared to the Western Transect of the ATLAS project (thin line in Alaska).

carbon balance, and the vegetation dynamics of the region through time on century to millennial year time-scales [*Brigham-Grette et al.*, 1998, 1999, 2001; *Nowaczyk et al.*, 2002]. Retrieval and interpretation of the full 3.6 million year core will be an enormous advance to our understanding of the Arctic's history.

[3] The NSF-LAII ATLAS (Arctic Transitions in Land-Atmosphere Systems) study of the Alaskan Arctic has provided us with both a model for study of the Russian Arctic and a basis for circumpolar comparisons and extrapolations by forming multiinvestigator collaborations to more fully understand the linkages and feedbacks between hydrology, meteorology, vegetation, snow, and gas fluxes. The ATLAS group has worked along the so-called Western Transect in Alaska (Figure 1), trending northeast from Council and Kougarok on the Seward Peninsula to Ivotuk in the interior to Barrow on the Arctic coast, with the general aim of making comparisons to the Kuparuk transect of the Flux studies [*Weller et al.*, 1995]. The proposed Northern Far East transect in Russia (ATLAS Synthesis Meeting, Victoria, BC, February 2001) trends northwest from Lavrentia (directly across the Bering Strait from the Seward Peninsula) to Lake El'gygytgyn in the interior to Cherskii on the Arctic Coast (Figure 1). Both transects have Arctic Ocean, Bering Sea, and interior analogs at roughly the same latitudes, but important differences exist between the two: they cross different climates and climate trends, and cross different ecosystems (described later). For example, the most northern Russian site is forested and the southern site is not, opposite to the Western Transect in Alaska. Our work focuses on the interior point of the Russian transect at Lake El'gygytgyn. Using the sediment core for temporal extrapolations and the Northern Far East transect for spatial extrapolation, our overall goals is to paint a more complete picture of the hydrological cycle, biogeochemical cycles, paleoenvironmental dynamics, and energy balance of this region. This paper presents the results of our remote sensing and modeling research on Lake E's modern ice cover dynamics and their implications for the core interpretation.

1.2. Prior Research: Lake El'gygytgyn's Climate Record and the Significance of Lake Ice

[4] In May 1998, we successfully collected 23 m of core in overlapping sections from the center of Lake El'gygytgyn, penetrating nearly 13 m of sediment (Figure 2, white cross). The cores have since been analyzed for all standard climate proxies (including diatoms, pollen, magnetic sus-

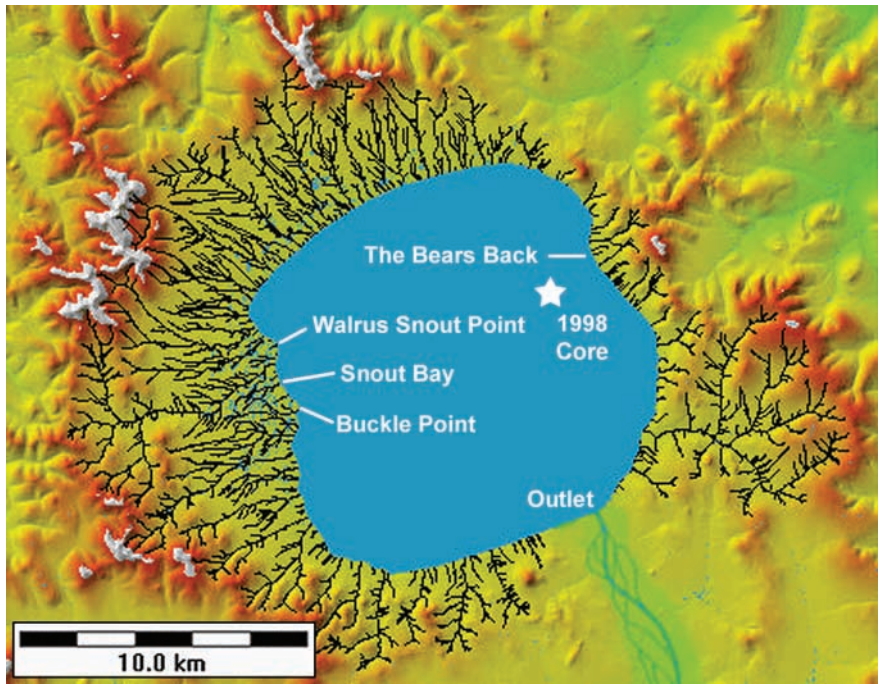

Figure 2. Lake El'gygytgyn. Shown here is color-coded topography of El'gygytgyn Crater with computer modeled stream channels (black lines). The lake is approximately 12 km across, and sits off-center in the 18 km wide crater. The white cross is the location of a core retrieved in 1998. Watershed elevation ranges from 492 m at lake surface to 906 m at crater rim.

ceptibility, etc), and have been dated via optically stimulated luminescence (OSL) and ^{14}C methods [*Brigham-Grette et al.*, 1998, 1999; *Cosby et al.*, 2000; *Brigham-Grette et al.*, 2001; *Nowaczyk et al.*, 2002]. This core has been found to record the Younger Dryas (YD) event, stronger Dansgaard/Oeschger-Henrich tandems but especially D/O interstadials 19 and 20, an inter-stage 5d event, and the "YD-like" event at the stage 5/6 transition, as well as strong millennial scale teleconnections with the $\delta^{18}O$ stable isotopic record from Greenland GISP Ice Core. Notably, the core contains the best resolved record of the last interglacial with all of its substages 5a through 5e and is the longest terrestrial Arctic paleoclimate record yet recovered, recording climate changes over the past 300,000 years; another 3.3 million years of record awaits coring.

[5] The core proxy measurements reveal that the timing and duration of the lake ice cover is perhaps the key environmental variable driving differences in sedimentation, biological productivity, and organic matter preservation through time. *Brigham-Grette et al.* [2001] proposed that the response of Lake El'gygytgyn to changing regional climate can be modeled between the two conceptual modes, indicative of an interglacial-type environment characterized by an open-water summer season and a glacial-type environment characterized by the lack of an open-water season. These modes are not limited only to true glacial and interglacial conditions, but also to warm periods during true glacial times and cold periods during true interglacial periods. The interglacial mode is described by generally oxic conditions, suggesting that the lake water was well mixed and had a long open water season. The glacial mode is described by anoxic conditions (at least at the sediment/water interface), likely caused by lake ice that did not completely melt in the summer, limiting wind-induced waves and seiches and perhaps encouraging thermal and chemical stratification. "El'gygytgyn" is a Siberian Chukchi phrase that means "white lake", indicating that it may have remained ice-covered year-round in historic times. Because the dynamics of lake has played such a significant role in the biogeochemistry of this lake throughout history, much of our modern process research is centered around understanding these dynamics and their relation to the rest of the system, so that we can better hindcast paleoclimate.

[6] Lake ice affects the thermal and mechanical controls of the atmospheric driving variables (radiation, wind, and air temperature) on the water, as well as the formation of thermal bars and currents within the lake. These controls and currents must be understood before a proper interpretation of the core can occur. Changes in water density within the lake are likely due almost exclusively to changes in temperature, as the salt content of the water is very low and varies little with depth. These temperature increases are the result of direct heating of the lake water and sediments by the Sun and by the addition of warm stream water. Our research in 2000 revealed that the underwater shelves likely play an important role in warming and mixing the lake (Nolan, unpublished data) in the following way. The water near the center of the lake (Figure 2, white cross) ranged from 3.08° to 2.88°C from top to bottom at the beginning of measurements in mid-August; when pressure differences are taken into account, the density of the water is nearly uniform throughout the water column, allowing free mixing. The entire water column at the lake's center warmed uniformly (about 0.2°C) over two weeks of continuous measurements, except for the deepest part of the lake that warmed more quickly (about 0.3 C). The sediments of these shallow shelves (about 5 m deep) absorb solar energy, heating the overlying water to between 4° and 5°C (in mid-August).

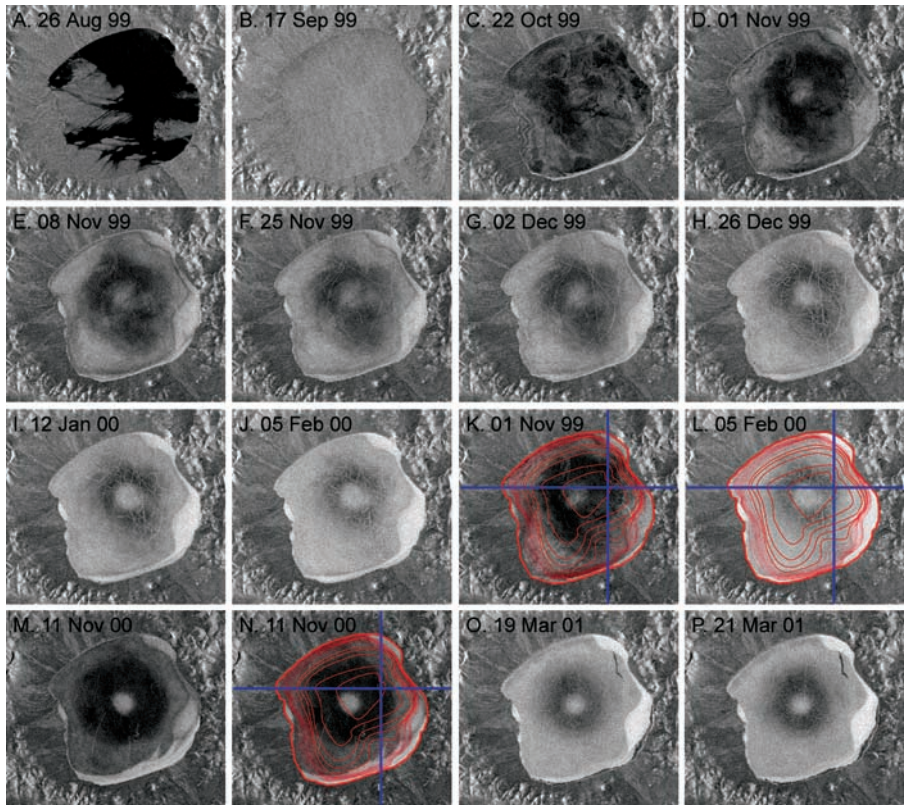

Figure 3. Lake ice formation and growth. All scenes are Radarsat Standard Beam 6. In **A** and **B**, wind effects can easily be confused with ice formation, especially in late fall. The onset of ice formation, **C**, is denoted by the presence of cracks and mottled backscatter but no bullseye pattern, indicating that this pattern is not related to a quirk of the freeze up process. Within a week of ice formation, trends in the bullseye pattern are already apparent in **D**. The sequence in **E**–**J** shows the development in this bullseye pattern, and strongly suggests that the pattern is an ongoing process related to bubble entrainment. The variations in this pattern are strongly related to bathymetry, as seen in **K** and **L**; contour interval is 10 m, with the deepest contour at 170 m and shoreline (0 m) outlined with thick red line. The blue cross is the location of a core taken in 1998. In **M**, notice the two week old ice cover in winter 2000–2001 shows a clearly circular bullseye pattern, suggestive of an underlying cone structure. Bathymetric contours are laid over this scene in **N**, and show the bright spot concentrated in the deepest few meters of the lake; it may not be a coincidence that the deepest spot is located directly above the cone, as described in the text. In **O** and **P**, snow-ice formation is seen to occur as cracks develop in midwinter and allow somewhat pressurized lake water to seep onto the ice surface; these effects due to liquid water fade away completely once the water refreezes within the snow.

As this water warms in spring and approaches 4°C (maximum water density), it likely sinks and begins a density-driven current off the shelf and down to the deepest parts of the lake [*Hobbie*, 1984; *Lehman et al.*, 1995; *Wetzel*, 2001] that lasts throughout the summer. While the lake remains covered with ice and snow, however, the thermal energy of the shelf water likely diffuses faster than the water can sink, creating a thermal bar that prevents mixing. Once enough shelf water sufficiently warms, this bar is broken and the shelf water travels to the bottom of the lake, carrying nutrients, diatoms, gasses, and sediments with it. These flows play an important role in our interpretations later in this paper.

2. Lake Ice Observations

[7] We have used a combination of space-borne remote sensing instruments to study lake ice dynamics on Lake E, including ERS-2, Radarsat-1 and Landsat 7. We have acquired over 400 synthetic aperture radar (SAR) scenes since 1998, which were then terrain corrected using a Digital Elevation Model (DEM) created from Russian topographic maps and software from the Alaska SAR Facility (ASF). We obtained 4 Landsat-7 images from 2000, two of which show details of lake ice breakup; we also obtained another 20 low-resolution browse scenes from 1999 to 2001 to increase temporal resolution. This section describes our observations of the dynamics and timing of ice formation in winter, snowmelt on the lake ice in spring, and lake ice decay in summer.

2.1. Ice Growth Mechanisms

[8] The initial presence of ice is most easily confirmed by the presence of linear features on the lake surface interpreted as cracks, leads or floes in the ice (Figure 3c). Partial ice formation in early stages was difficult to observe because it occasionally had a similar appearance to wind ripples (Fig-

ures 3a–3b). An ice skim can form on nearly any date during the open water season if the conditions are right—a calm, clear, cold night; we in fact observed a short-lived skim on 10 August 2000 while conducting seismic work through the night. Our research shows that a permanent, complete ice cover will not form at Lake E until late October.

[9] Beginning shortly after the first indication of ice formation, we observed a pattern within the ice that gradually became more pronounced throughout the ice growth season (Figures 3d–3j). This nearly identical pattern is repeated in every winter of observation, and so is not simply due to some random perturbation on the day the ice skim formed, such as snow-ice formation. Snow-ice forms as snow depresses the ice below water level, creating a slush that eventually freezes within the snowpack; our SAR observations show this occurring only occasionally and at a very localized level (Figures 3o and 3p). In contrast to how snow-ice forms, these broad-scale spatial features are largely concentric circles reminiscent of a bull's-eye target, and have been given the identifying numbers 1, 2, 3 and 4, with the high number located at the lake center (Figure 4a). Because the winter snow in the Arctic is dry, the vast majority of SAR microwave energy transmits through it [*Rott and Nagler*, 1994], indicating that this backscatter pattern is certainly a function of the spatial differences of scatterers within the ice.

[10] Figures 3d–3j and Figure 4 reveal that all of the ice regions continue to increase in backscatter through the winter, indicating an ongoing process, such as bubble entrainment as the ice grows thicker from below. The fact that the bull's-eye pattern is not present at ice freeze-up in any year, but only after about a week of ice growth, is further support for bubble entrapment. Figures 4b and 4d show this gradually brightening for the shelf ice (type 1). As the season progresses in late winter, the brightening stops for likely several reasons: ice growth is slowing, most of the energy is already being reflected back by the upper layers, and the returned signal is nearing saturation. Figure 4c shows a close-up view of this late-winter slow down for the shelf ice. As can be seen, each beam mode has a characteristically different signal strength, but the differences between the ascending and descending passes for a particular beam mode are slight, as might be expected for backscatter from a flat surface with no preferential direction of scatterers. The varying response of the different beam modes is largely due to the difference in incidence angle—the energy transmitted into the ice reflects differently from the same scatterers (that is, bubbles, such as in Figure 5) because it enters at a different angle.

[11] We have found that the ratios of the different beam modes can be used to discriminate the different ice types better than the backscatter value alone (Figure 4e). For each ice type, we selected between 0.66 to 3.8 km^2 area and found the mean Data Number (DN) for each beam mode (combining ascending and descending data for that beam mode) for that area over the range of dates shown in Figure 4c, when the response was fairly linear with time. We then divided this mean response from ERS-2 by the mean response from each of the 7 Radarsat beam modes to create Figure 4e. These ratios are expressed in decibels, and show that each ice type has a unique signature, likely due to differing size, shape or orientation of the scatterers. Once field work is completed on the actual bubble morphology of these ice types, these ratios may prove valuable to analysis of biological productivity at other lake systems.

[12] Variations in SAR backscatter across Arctic lakes have been observed previously, and generally attributed to one of two processes (during winter): the ice freezing to the bed or bubbles in the ice [*Weeks et al.*, 1977; *Jeffries et al.*, 1994, 1996; *Kozlenko and Jeffries*, 1999]. When ice freezes to the bed, its backscatter drops abruptly, as the microwaves are then reflecting from an ice/land interface rather than an ice/water interface. Clearly this can only occur in shallow lakes, and cannot account for the variations we see. Variations in backscatter from ice not grounded were generally much weaker than observed on Lake El'gygytgyn. *Jeffries et al.* [1994] found that ungrounded ice increased in backscatter throughout the winter due to the continued entrainment of bubbles. They used a simple lake ice model to show that the maximum backscatter can be reached in only a few centimeters of ice if enough tubular shaped bubbles are present. By examining the ice itself, they were also able to distinguish different bubble morphologies resulting from different genesis mechanisms that presumably would affect backscattering in different ways. Therefore prior research also suggests that the morphological differences we observe on Lake El'gygytgyn are due to not only to the spatial distribution of bubble content by volume, but also their distribution of bubble shape, size, and orientation.

2.2. Snowmelt Mechanisms

[13] Because of the large difference in the dielectric properties of dry snow and liquid water, the *onset* of melt is unambiguously recorded in the SAR scenes of El'gygytgyn's lake ice. *Rott and Nagler* [1994] showed that C-band SAR microwaves can penetrate dry snow as deeply as 20m, but when even 3% of liquid water is present this penetration depth decreases to less than a wavelength (about 5 cm). It is clear therefore that for most of the winter, the changes we observe on the lake's surface are occurring in the ice, not the snow. Abruptly in spring, the bull's-eye pattern disappears and is replaced by a dark, mottled texture (Figures 6a–6d). This texture changes from scene to scene due to variations in snowmelt, and often turns completely black, indicating that at least the surface layers of the snowpack contain significant liquid water. Occasionally the familiar winter bull's-eye pattern returns completely, indicating a freezing event, or partially, indicating differential snowmelt. In general, snowmelt is earliest near the edges of the lake, probably due to the influence of snowmelt runoff from the crater rim and the warmer soil there. Figure 6e also shows a Landsat quicklook (a low resolution composite fixed at bands 5, 4, and 3) during the onset of snowmelt, which shows no obvious sign of melt. Here the SAR instrument is detecting water within the snowpack while the Landsat quicklook detects only snow, not whether it is melting.

[14] However, many details of the snowmelt process which are unapparent in SAR data are revealed by the full-data scenes (not quicklooks) of Landsat 7 toward the end of the melt season. The inability of SAR to give detailed information on the ongoing melt processes is well described [*Rott and Nagler*, 1994; *Konig et al.*, 2001]. Figure 6i shows a high-resolution Landsat 7 scene from 16 June 2000 (bands 5, 4, 3). Numerous runoff channels can be seen, some appearing to run from the terrestrial streams onto the ice

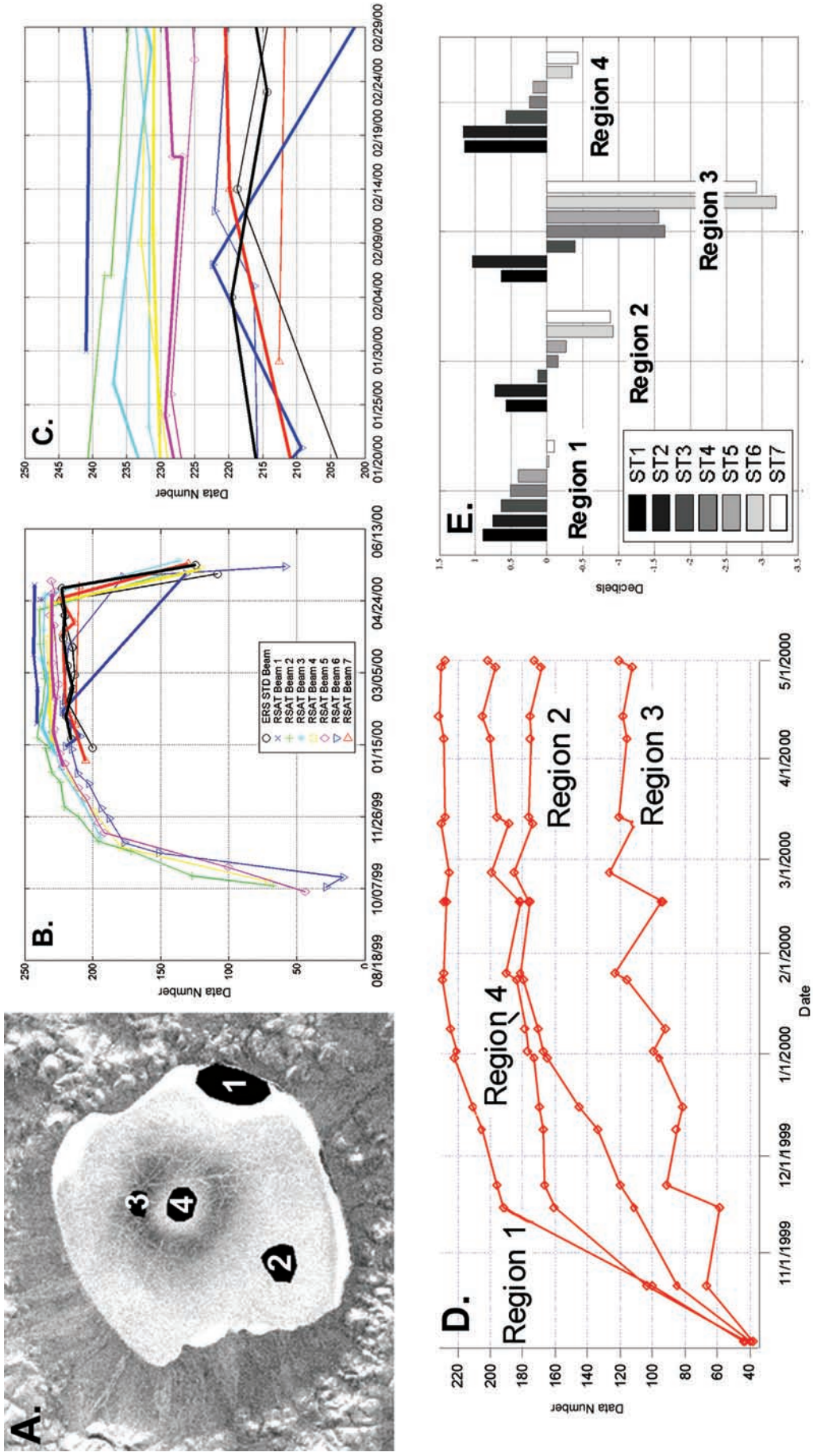

Figure 4. Differences in lake ice bubble content. Four distinct regions of backscatter are seen in the lake ice, labeled in **A** along with the actual polygons used for averages in **C** and **D**. In **B**, average lake backscatter for the 16 combinations of beam mode and ascending/descending orbits of ERS-2 and Radarsat-1 are shown; thick lines denote ascending and thin lines descending. A close up of the linear region is shown in **C**, which shows that differences between ascending and descending passes of a particular beam mode are slight, while appreciably differences exist between the beam modes themselves. Radarsat standard beam four is shown in **D** for all ice types for comparisons. A ratio of ERS to each of the 7 Radarsat beam modes is shown in **E** for the dates range used in **C**. Note that the ice regions can be discriminated based on these ratios.

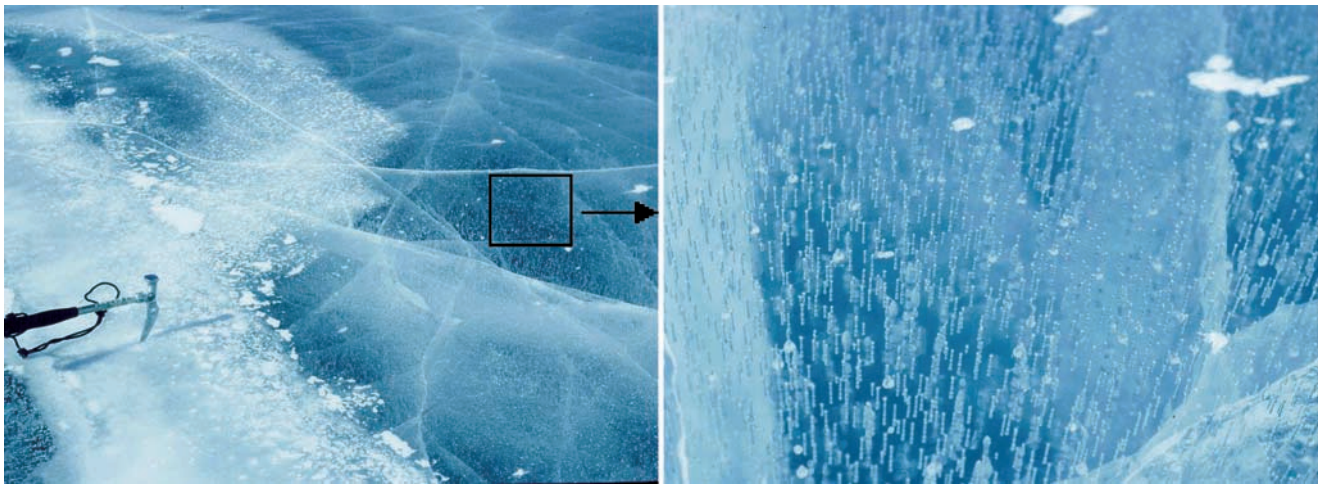

Figure 5. Bubbles and leads in lake ice. A refrozen crack is seen at left; at right are bubbles entrained in the ice. These photos were taken in the bare ice region on the north end of the lake in May 1998. The photo at right is approximately the size of the square at left (about 30 cm across). This ice is likely characteristic of ice region 2, though no systematic observations have been made.

surface. Snow and ice can generally be discriminated by the absence of cracks and the slightly bluer color of ice. Compare this to an ERS-2 scene taken about a week later (Figure 6j). Here it can be seen that in many areas the boundaries between ice and snow can be traced nearly identically in both, with the darker areas in the SAR scene relating to the bluer areas in the Landsat scene. This same trend can be seen in other comparisons in the late melt season. But Landsat quicklooks can also discriminate snow from ice, at a lower spatial resolution, with their main

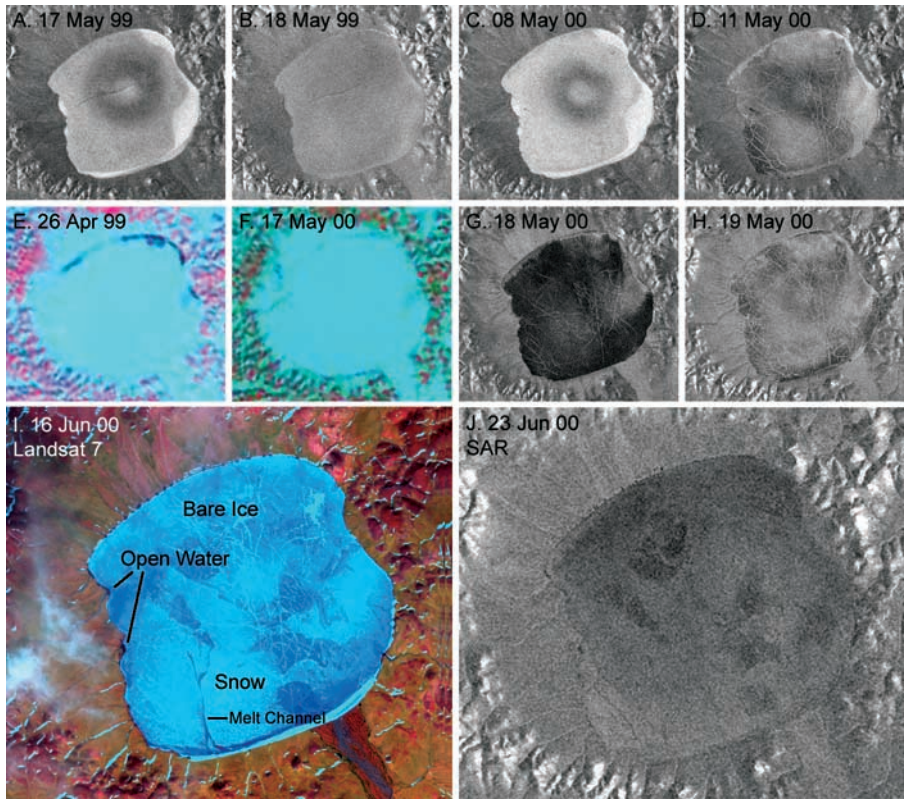

Figure 6. Snow melt on lake ice. Compare **A&B** to **C&D** for onset of snow melt—a few percent liquid water in the snowpack decreases the penetration depth of SAR such that the bullseye pattern within the ice can no longer be seen. The Landsat 7 quicklook in **E** shows a snow free area due to wind scour before melt (note year). SAR scene in **G** shows strong melting event, followed the next day by less, but continued, melt. Landsat 7 in **I** shows evidence of bare ice, but little evidence of melt within the snowpack as does the SAR scene acquired a few days later in **J**.

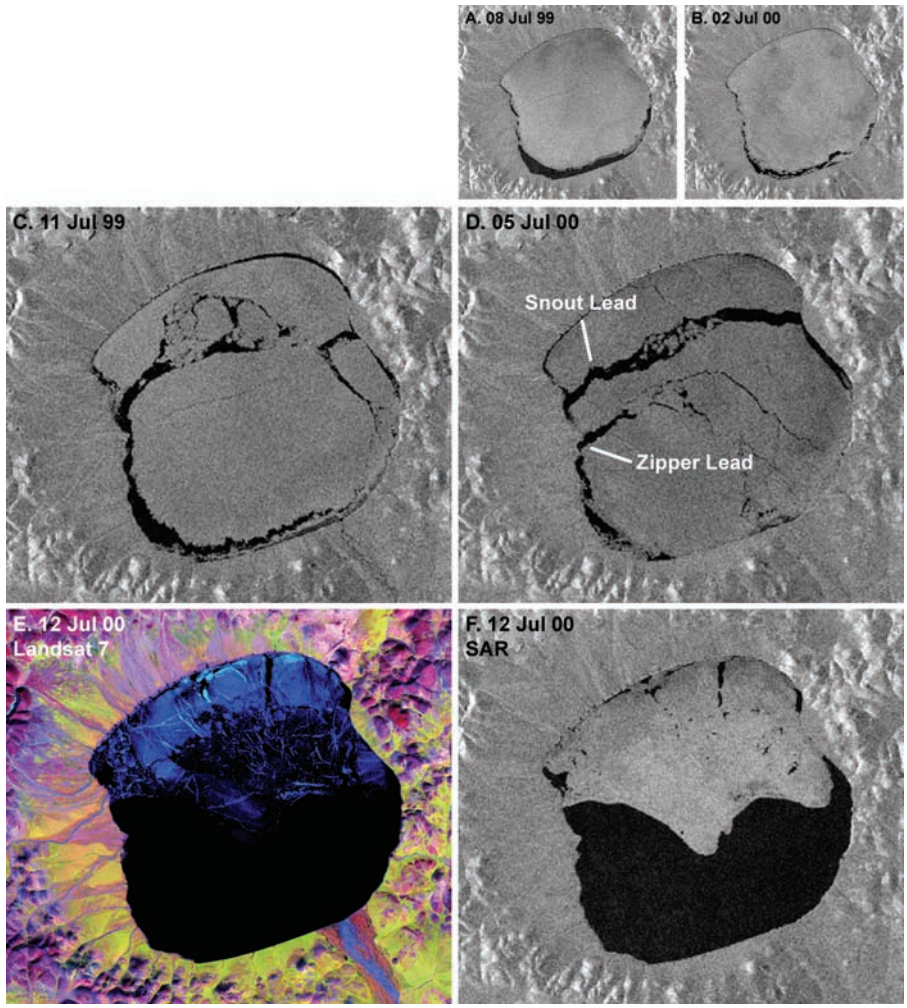

Figure 7. Lake ice breakup. Compare **A**&**C** to **B**&**D** to note similarities in breakup between two winters from SAR. First a moat forms, allowing the ice to shift with the wind. Then leads open at two prominent points of land on the west shore. And finally the ice breaks into floes that allow the entire mass to shift freely, facilitating breakup. The last few days of breakup in 2000 were captured nearly simultaneously with Landsat and SAR on 12 July in **E** and **F**.

advantage being that they are free. Using these quicklooks (e.g., Figure 6d), we found that snow cover on the ice throughout the winter is not uniformly distributed—about 5% of the total ice surface at the north end of the lake was scoured free of snow by the wind in winter 1998–1999 and about 1% in winter 1999–2000, with less than 0.05% error (determined from pixel size as percentage of total area) for a particular scene. Our winter 1998 field trip provides ground truth showing that a similar state existed then as well. However, none of the SAR scenes reveal this snow-free area during winter because the signal penetrates dry snow with little backscatter, just as if it were not there. Therefore, while Landsat provides a more visually satisfying image and easily discriminates snow from ice, SAR is better suited for detecting snowmelt onset.

2.3. Ice-Melt Mechanisms

[15] Snowmelt ends completely sometime in late June, when the ice itself becomes fully exposed and subject to surface melt. During this time, the ice in SAR scenes appears a nearly uniform gray with little variation in backscatter either spatially or temporally, and with no further signs of the bull's-eye pattern (Figure 7). The absence of the bull's-eye indicates that either the penetration depth has been severely reduced or that the dominant body scatterers have changed. Both are likely the case. Because of the diurnal thawing and refreezing on the ice surface, it becomes porous and opaque, trapping liquid water and air, decreasing the penetration depth. Also, the body of the ice takes on liquid water from melt at the grain boundaries long before the interiors of the grains, creating "candle ice", which would significantly change the scattering mechanisms.

[16] Our measurements of lake ice melt are limited to measurements of ice-covered area. *Jeffries et al.* [1994, 1996] and *Weeks et al.* [1977] were able to measure lake ice thickness change directly with SAR, due to the difference in backscatter when the ice freezes to the lake-bed; Lake El'gygytgyn is too deep for this method. The first area of the lake to open up is a moat along the edges. The first

Table 1. Important Dates of Lake Ice Dynamics Derived From SAR

Winter	Onset of Lake Ice Freezing	Onset of Lake Ice Snowmelt	Onset of Lake Ice Moat Formation	Completion of Lake Ice Melt
1997–1998	No Data	<8 July	<8 July	8 July–9 August
1998–1999	>6 October	17 May–18 May	24 June–4 July	28 July–13 August
1999–2000	16 October–19 October	8 May–11 May	23 June–2 July	16 July–19 July
2000–2001	18 October–20 October	14 May–17 May	20 June–23 June	13 July–17 July

definitive signs of this moat from SAR typically occur in late June. Pools of liquid water are seen surrounding the lake in early June, however they cannot be distinguished from snowmelt ponds. Landsat, which can clearly discriminate water from wet snow, shows moat formation occurring in Snout Bay (Figure 2) as early as mid-June (Figure 6i). The moat gradually widens and extends around the entire lake, but the south shore generally widens much more quickly, likely due to the presence of shallow shelves that create warmer water in this area.

[17] Once the moat extends around either the north or south shores, the ice is free to move slightly in the dominant wind direction, which is nearly north-south, placing increased stress on shoreline pinning points. The most important of these are Walrus Snout point, Buckle Point, and the Bears Back (Figure 2). These points of land pinch the lake, and therefore the ice, along an east-west direction. Field observations from summer of 2000 show ice-shoved gravel piles up to 4 m high at Buckle Point, the highest anywhere on the shore. As might be expected, these points act as initiation points for leads. Figure 7 shows the formation and widening the Snout and Zipper leads. The Zipper lead, emanating from Buckle Point, typically opens first, though has a tendency to close and reopen before the Snout lead is formed. That is, the Zipper lead alone is not enough to free the ice from Snout Bay and the northwest corner, which occurs when the Snout lead finally opens. It is clear that in some years the Zipper opens, or at least cracks, *before* snowmelt is finished (Figure 6a), indicating that wind stress even without a moat is strong enough to initiate cracks there. Shortly after both leads are open, the ice between them disintegrates and provides enough open water for individual floes to form and let the entire ice mass to be freely shifted by the wind and destroyed by wave action and melting.

[18] These leads formed during each of the first three winters of observation at roughly the same locations, but the winter of 2000–2001 revealed a characteristically different pattern. In this spring, the moat widened considerably faster in the south-western corner of the lake, allowing the ice pack free movement past Buckle Point. Thus the typical leads did not form. Instead a lead in the north–south direction opened across the entire lake, through the center of ice region 4 (Figure 4a). Ice melt proceeded similar to prior years after this point, with large floes breaking into smaller ones that were then destroyed by wave action.

2.4. Timing of Events

[19] Table 1 presents a summary of the SAR observations for the past 4 winters. Snowmelt on the lake surface begins in May and ends in June. Ice melt begins during snowmelt, but the total ice surface area does not begin to decrease until late June or early July, as denoted by the presence of a moat. Complete ice loss does not occur until mid-July or early August. The date ranges in Table 1 denote the "before" and "after" images bracketing the event (e.g., no sign of snowmelt was present on 8 May 2000, but the next image acquired, on 11 May, shows melt).

[20] These data are significant not only for climate change studies related to the sediment cores, but for the coring effort itself. To recover the full 3.6 million year core, we will need to use more than 10 tons of equipment related to drilling, which must be transported across the ice and supported by it. Using Table 1 as a guide, we should plan to remove this equipment by May 8th at the latest for transportation across dry snow, though the ice will be stable enough to support the weight for perhaps another 6 weeks.

3. Lake Ice Modeling

[21] Our study of the current lake ice dynamics of Lake El'gygytgyn is largely driven by our desire to better interpret the sediment core record we recovered from the lake-bed in 1998. To extend our remote sensing observations to time periods that are not covered by remote sensing data sets (hindcasts or forecasts), our approach is to apply a physically based lake and lake ice model to the current climate system using our remote sensing to validate the model performance. In future work we will use this locally validated model along with core proxy records to determine paleoclimate conditions.

[22] Our validation effort uses a globally gridded data set for model input, since there were no local meteorological observations in the crater before our field work in summer 2000. We used data from the National Centers for Environmental Prediction (NCEP) reanalysis [*Kalnay et al.*, 1996]. These represent "snapshots" of the state of the atmosphere on a six-hourly basis on a 2.5 $\times$ 2.5 degree grid and are compiled through optimally blending output from a global numerical weather prediction model with observed data. The Climate Diagnostics Center (CDC) (Boulder, Colorado) holds archives from the NCEP reanalysis for the late 1940s through the present. Because the full energy balance input data are not available here, the model's weather input consisted only of air temperature.

[23] We used a one-dimensional, physically based model [*Liston and Hall*, 1995a, 1995b], composed of four major submodels. First, a surface-energy balance submodel determines the surface temperature and energy available for freezing or melting. Second, a lake mixing, energy-transport submodel describes the summer evolution of lake-water temperature and stratification; ice is initiated when the upper-lake temperature falls below freezing. Third, a snow submodel describes the snow depth and density as it accumulates, metamorphoses, and melts on top of the lake ice. Fourth, a lake ice growth submodel produces ice by two

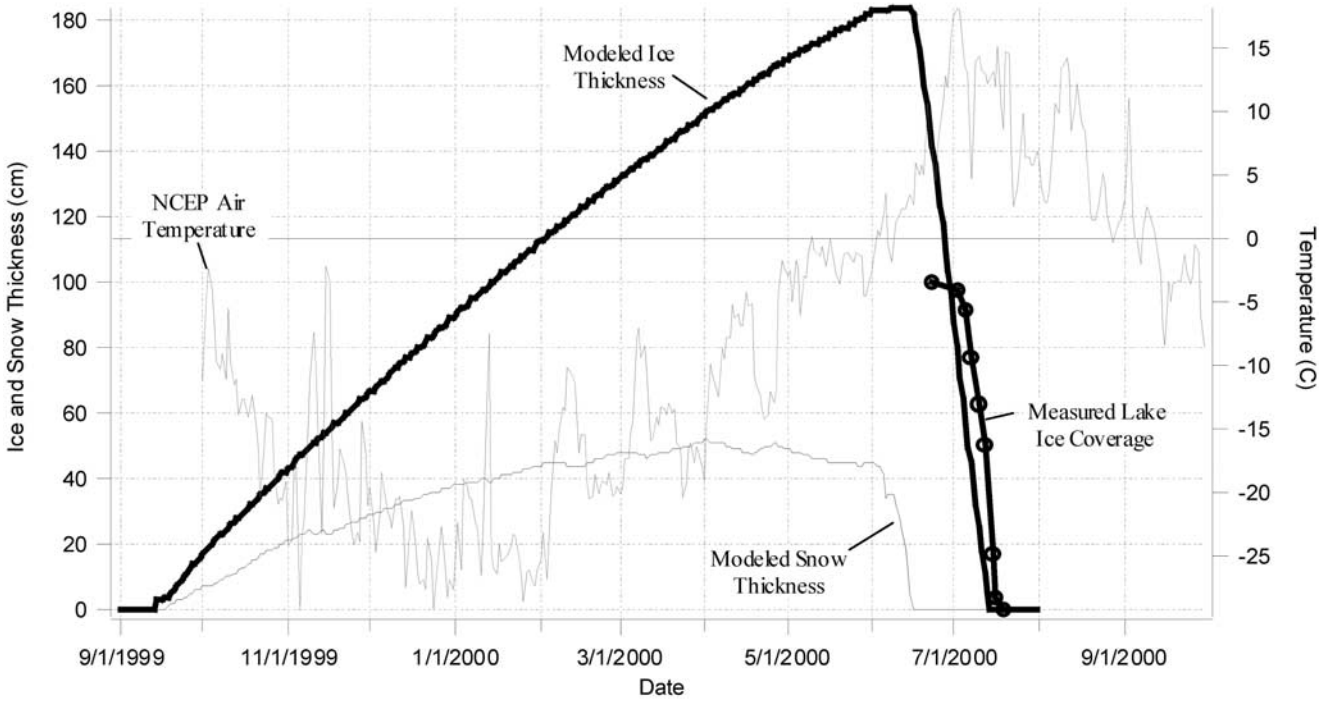

Figure 8. Lake ice modeling. Local air temperature data derived from the NCEP reanalysis was used to drive a 1-D model of lake ice growth and and melt. Snow thickness was varied gradually over the winter to a maximum of 50 cm. The modeled ice thickness decrease in spring corresponds well with the measured lake ice coverage (given as a percentage of total lake ice area, using thickness axis).

different mechanisms: (a) relatively bubble-free clear ice grows at the ice/water interface due to thermal gradients within the ice, and (b) snow-ice forms at the lake ice surface from the freezing of water-saturated snow or slush; this slush can come from the upwelling of water due to an overburden of snow, from snowmelt, or from rain on snow. When the surface energy balance is coupled to the lake, lake ice, and snow submodels, it provides the surface temperature boundary condition which forces lake water temperatures, lake ice growth, and snow accumulation and metamorphism. Key model output includes the dates of initial ice freeze-up and breakup, and the end-of-season clear-ice, snow-ice, and total ice depths, and date of complete removal of the ice cover [*Magnusson et al.*, 2000].

[24] As can be seen from Figure 8, the model output is in good agreement with the SAR/Landsat observations, especially given that we used modeled input data. Based on our observations in winter of 1998, we found that the snow cover distribution linearly ranged from zero at the north end of the lake to about 1 m at the south end. Therefore, in this one-dimensional model, we used an average snow thickness of 0.5 m, with snow being added gradually throughout the winter. Modeled ice cover formation precedes the observations by several weeks, largely because the model has no local data on wind speeds or net radiation, the two dominant drivers of this timing; such data will greatly improve this correlation when available. The timing of snow and ice *melt* depend much less on specific wind and radiation data, and here we the see the model and observations agree to within several days. Note when comparing lake ice breakup evolution between modeled and observed curves that the one-dimensional model outputs ice-loss by thickness only, while the observed ice-loss is reported as a percentage of area only. Thus, ice melt is likely beginning *before* moat formation, but this cannot be observed from SAR. Given the strong correlation between modeled and observed timing, and its prior history of success [*Liston and Hall*, 1995a, 1995b; *Jeffries et al.*, 1996], we are now confident that this model can be extended to hindcast these dynamics for time periods not covered by remote-sensing data sets.

4. Discussion

4.1. Possible Origins of the Bull's-eye Pattern

[25] The SAR backscatter variations are definitely due to variation in bubble content or morphology, but it is less clear and more interesting to determine what causes the variations in bubbles themselves. The margins of the lake are surrounded in places by a shelf with a shallow slope which, in general, breaks more steeply at about 10 m—ice region 1 mimics this shelf area as best as we know its boundaries. We have found that a bathymetric map obtained from Russian sources charts these shelves fairly well based on field observations, and Figures 3k–3l reveal the strong correspondence. The sandy sediments on these shelves are significantly warmer (about 1°C) than sediments elsewhere because they receive significantly more solar radiation (Nolan, unpublished data). The shelf sediments therefore should support more life, which consequently must respire and decompose, creating bubbles during winter. In the remaining discussion, we follow *Wetzel*'s [2001, p. 150] definition of biological "production" as "a flow or flux of

mass or energy over time and has the dimensions of mass per area formed over a period of time and includes any losses from respiration, excretion, secretion, injury, death, and grazing''; we use the term ''biological productivity'' analogously with production, though more to describe the process than the rate itself.

[26] Given that the high backscatter of ice region 1 seems clearly due to increased biological productivity and that the most reasonable explanation for variation in body scatterers in lake ice is the bubble content, it is likely that the remaining variations in backscatter (region 2, 34) are due to variations in biological production beneath them as well. Region 3 possesses the least number of bubbles and initially covers nearly all of the flat lake bottom (Figures 3k and 3n). By the end of winter, however, this region is limited to a ring around ice region 4, giving the appearance that region 2 has ''stolen'' area from region 3. In actuality, this apparent spread of region 2 into region 3 is likely due to differences in lake bed production within region 3, with the darkest areas remaining at end of winter likely indicating the least productive areas of the entire lake bed.

[27] We have identified several potential mechanisms for the anomalously high concentration of bubbles in the center of the lake (region 4):

1. *Density Currents*. It is likely that warm (4°C), dense water currents flow from the shelves down to the deepest part of the lake, possibly carrying either enriched or depleted dissolved oxygen and nutrients, depending on the level of productivity on the shelves [*Hobbie*, 1984; *Lehman et al.*, 1995; *Wetzel*, 2001]. While measurements of production have not yet been made, the lack of any visible algal growth on the shelves suggests that the downward flowing water is likely rich in dissolved oxygen and nutrients. From Figures 3l and 3n, it is clear that ice region 4 lies above the deepest part of the lake. We therefore expect this warm, nutrient-rich pocket to become more productive and therefore generate more bubbles, causing the bull's-eye effect in a relatively less productive region of sediments. The water displaced by this warm water is the coldest in the lake at 3.3°C in late summer. This displaced water would tend to cool the surrounding sediments in an annular pattern, further decreasing its productivity compared to the deep pocket, creating the low backscatter region 3. Given that the shelf area is only 1°C warmer than elsewhere in the lake and has significantly higher productivity, it would appear that even small temperature differences (perhaps ~0.1°C) can have a large impact on biological production at these low temperatures.

2. *Sediment temperature*. Ice region 4 may indicate the location of the central peak of the impact crater; such peaks are a feature of large meteorite craters such as this one. Though our current seismic measurements cannot pinpoint the exact location of this bedrock peak because the measurements did not penetrate deeply enough, its presence can be inferred from the draping patterns in the sediment stratigraphy [*Niessen et al.*, 2000] and is located about 500 m directly beneath ice region 4. Because the sediments are thinner on top of this peak than the area immediately surrounding it, they will likely be warmer due to the relative increase in geothermal heat transfer (note that this is not the same as the peak itself radiating remnant heat from the impact, which has long since been lost). That is, all else being equal, one would expect the warmest part of the sediment floor to be directly above the peak and the coolest to be above the annular sediment filled valley surrounding the peak. This effect would cause a variation in biological production and therefore bubble production. Though these peaks are typically found in the center of the crater, oblique impacts and grossly irregularly preimpact topography or substrate can cause them to be offset.

3. *Groundwater or gasses*. The sediments draped over this peak may also act as an anticlinal gas trap, focusing gas bubbles or groundwater from below toward this peak. Because of its large thermal mass, Lake E sits above an open talik, meaning that no permafrost likely exists beneath. However, permafrost exists continuously for hundreds and thousands of kilometers around it. Because of its impact origin, the igneous rock beneath it is highly shattered, and would make an easy conduit for groundwater or melting hydrates to percolate upwards. Once within the sediments, the draping pattern would tend to focus this mass flux toward the top of the anticline, directly above the peak and beneath ice region 4. Preliminary seismic evidence supports this mechanism, as described below.

4. *Circus tenting*. If one of the above mechanisms caused more bubbles to accumulate in the center ice during its initial formation, this ice would be less dense and ride higher in the water than the surrounding ice, like the cover to a circus tent. The underside of this ice might also grow more slowly because of the increased insulation of the more bubbly ice above it. The resulting conical rise at the water/ice interface at center might then act like self-reinforcing attractor for bubbles rising under other parts of the lake, because these bubbles would travel upwards and therefore toward the center. While the brightening observed throughout the winter would then be an artifact of an interface process, this process still requires a trigger from a source near the bottom of the lake. Also, the low bubble-content annulus surrounding region 4 indicates that such a tenting process is localized to outer boundary of region 3.

[28] Evidence that some *combination* of these mechanisms may be at work is revealed by contrasting scenes from winter 1999–2000 (Figures 3c–3l) and winter 2000–2001 (Figures 3m–3p). As can be seen in Figure 3m, the distribution of ice regions 3 and 4 in winter 2000–2001 were much more circular than the previous winter (as well as winter 1998–1999, not shown). Ice region 4 is also slightly smaller than in the previous year. It may be that the 2000–2001 winter scenes are dominated by a process related to the central peak (mechanisms 2 and 3), rather than shelf-water heating (mechanism 1) as in the previous two winters. In this scenario, mechanisms 2 or 3 are base effects that are relatively insensitive to climatically driven changes in lake temperature, with the density flows adding bubbles in warmer or sunnier years. Only more geophysical field work can conclusively prove or disprove these hypotheses; such work is planned.

4.2. Implications for Paleoclimate Research

[29] Both our research and seismic measurements support the fact that the deepest part of the lake is nearly directly above central peak of the crater (roughly 350 m below the water/sediment interface), and this collocation may not be purely by chance. Considering the possibility that the sediments above the peak have been more biologically produc-

tive than the surrounding area for a long time (possibly millions of years), it is conceivable that they may be slightly more consolidated, if for no other reason than upward mass loss through bubble formation. It is also conceivable that gas or water percolating up from below throughout time would further tend to differentially consolidate the sediments in this location. There is some seismic evidence for both this consolidation and for piping structures between the peak and lake bed, though more measurements are required to conclusively verify this. This consolidation and bed-deepening process would then reinforce increased attraction of the warmer shelf-water there, further enhancing the biological production and further consolidating the sediments.

[30] That a region of higher biological production may exist in the region of interest for future sediment cores is significant, because this production can significantly change the nature of the sediments after they are deposited. For instance, the 1998 core shows clear changes between oxic and anoxic conditions. This core location is near the outer boundary of ice region 3 (Figure 3, blue cross), suggesting it is an area of lower productivity than the deepest part of the lake. During glacial summers, it is possible that a moat formed even though the ice did not completely break up, such that oxygen could be replenished here and then carried down to the deepest part of the lake with the density-driven current from the relatively warmer shelves. Thus a core taken in ice region 4 may show a somewhat different oxic/anoxic signature throughout the entire core than the core taken in region 3. This further suggests that cores taken in both locations will help us paint a more complete picture of the paleoenvironment than cores from only a single location, since the productivity of both regions have identical atmospheric drivers.

5. Conclusions

[31] Spaceborne SAR is a powerful tool for understanding the dynamics of lake ice formation, morphology, and melting, and this information has given us many important clues that will aid in the interpretation of our sediment core proxies from Lake El'gygytgyn. We were able to determine dates for lake ice formation, snowmelt, and ice melt to within a few days for each of the past four winters. We were able to model the timing of these events fairly accurately using only air temperature to drive a one-dimensional lake ice model. Bubble content and morphology of the ice were also found to vary spatially and temporally, and this has important implications toward our paleoclimatic interpretations of sediment cores taken from this lake.

[32] **Acknowledgments.** This material is based upon work supported by the National Science Foundation under Grant 0075122 to MAN and Grant 9905813 to JBG. Support was also provided by NASA under Grant NAG5-8722 from the Joint U.S.–Russian Research in Space Sciences Program (JURRISS) to VLS. Any opinions, findings, and conclusions or recommendations expressed in this material are those of the authors and do not necessarily reflect the views of the National Science Foundation or NASA. Support was also provided by the Alaska SAR Facility. ERS-2 is owned by the European Space Agency and Radarsat-1 is owned by Radarsat International, who hold copyrights on all data acquired.

References

Brigham-Grette, J., and L. D. Carter, Pliocene marine transgressions of northern Alaska: Circumarctic correlations and paleoclimate, *Arctic*, *43*, 74–89, 1992.

Brigham-Grette, J., et al., Preliminary lake coring results from El'gygytgyn Crater, Eastern Siberia, *Eos Trans. AGU*, *79*(45), F477, 1998.

Brigham-Grette, J., et al., Paleoclimate record of El'gygytgyn Crater Lake, NE Siberia—Pilot cores extended to 200 ka, *Paleoclim. Arct. Lakes Estuar. Newsl.*, *7*(Summer), 7, 1999.

Brigham-Grette, J., C. Cosby, M. Apfelbaum, and M. Nolan, The lake El'gygytgyn sediment core—A 300 ka climate record from the terrestrial Arctic, *Eos Trans. AGU*, *82*(48), F752, 2001.

Chapman, W. L., and J. E. Walsh, Recent variations of sea-ice and air temperatures in high latitudes, *Bull. Am. Meteorol. Soc.*, *74*(1), 33, 1993.

Cosby, C., J. Brigham-Grette, and P. Francus, The IMPACT Project: Sedimentological studies of the paleoclimate record from El'gygytgyn Crater Lake, *Eos Trans. AGU*, *79*(45), F230, 2000.

Dence, M., The nature and significances of terrestrial impact structures, in *24th International Geological Congress Proceedings (Planetology)*, pp. 77–89, Montreal, 1972.

Dietz, R., and J. McHone, El'gygytgyn: Probably the world's largest meteorite crater, *Geology*, *4*, 391–392, 1976.

Glushkova, O., Geomorphology and history of relief development of El'gygytgyn Lake Region, in *The Nature of the El'gygytgyn Lake Hollow*, edited by V. F. B. a. I. A. Chereshnev, pp. 26–48, Magadan FEB, Russian Academy of Science, 1993.

Hobbie, J., Polar limnology, in *Lakes and Resevoir*, edited by F. Taub, pp. 63–105, Elsevier Sci., Amsterdam, 1984.

Jeffries, M., K. Morris, and W. F. Weeks, Structural and stratigraphic features and ERS 1 Synthetic Aperture Radar backscatter characteristics of ice growing on shallow lakes in NW Alaska, winter 1991–1992, *J. Geophys. Res.*, *99*(C11), 22,459–22,471, 1994.

Jeffries, M., K. Morris, and G. Liston, A method to determine lake depth and water availability on the North Slope of Alaska with space-borne imaging radar and numerical ice growth modelling, *Arctic*, *49*, 367–374, 1996.

Kalnay, E., et al., The NCEP/NCAR 40 year re-analysis project, *Bull. Am. Meteorol. Soc.*, *77*, 437–471, 1996.

Konig, M., W. Jan-Gunnar, and E. Isaksson, Measuring snow and glacier ice properties from satellite, *Rev. Geophys.*, *39*(1), 1–27, 2001.

Kozlenko, N., and M. Jeffries, Bathymetric mapping of shallow water in thaw lakes on the North Slope of Alaska with spaceborne imaging radar, *Arctic*, *53*, 306–316, 1999.

Layer, P., Argon-40/Argon-39 age of the El'gygytgyn impact event, Chukotka, Russia, *Meteorit. Planet. Sci.*, *35*, 591–599, 2000.

Lehman, A., D. Imboden, and J. Gat, *Physics and Chemistry of Lakes*, Springer-Verlag, New York, 1995.

Liston, G., and D. Hall, An energy balance model of lake-ice evolution, *J. Glaciol.*, *41*, 373–382, 1995a.

Liston, G., and D. Hall, Sensitivity of lake freeze-up and break-up to climate change: A physically based modelling study, *Ann. Glaciol.*, *21*, 387–393, 1995b.

Magnusson, J., et al., Historical trends in lake and river ice cover in the Northern Hemisphere, *Science*, *289*, 1743–1746, 2000.

Niessen, F., C. Kopsch, B. Wagner, M. Nolan, and J. Brigham-Grette, The IMPACT Project: Seismic investigations of Lake El'gygytgyn, NE Russia—Implications for sediment thickness and depositional environment, *Eos Trans. AGU*, *81*(48), F320, 2000.

Nowaczyk, N., et al., Magnetostratigraphic results from impact crater lake El'gygytgyn, north-eastern Siberia: A possibly 300 kyr long terrestrial paleoclimate record from the Arctic, *Geophys. J. Int.*, in press, 2002.

Rott, H., and T. Nagler, Capabilities of ERS-1 SAR for snow and glacier monitoring in alpine areas, in *Proceedings of the 2ndERS1 Symposium—Space at the Service of Our Environment, Hamburg Germany 11–14 October 1993*, SP-361, pp. 965–970, European Space Agency, Paris, 1994.

Weeks, W. F., P. Sellmann, and W. Campbell, Interesting features of radar imagery of ice-covered North Slope lakes, *J. Glaciol.*, *18*, 18–27, 1977.

Weller, G., F. C. Chapin, K. R. Everett, J. E. Hobbie, D. Kane, W. Oechel, C. L. Ping, W. S. Reeburgh, D. Walker, and J. Walsh, The Arctic Flux Study: A regional view of trace gas release, *J. Biogeogr.*, *22*, 365–374, 1995.

Wetzel, R., *Limnology: Lake and River Ecosystems*, 3rd ed., Academic, San Diego, Calif., 2001.

J. Brigham-Grette, University of Massachusetts Amherst, Amherst, MA, USA.

R. Huntzinger, M. Nolan, and P. Prokein, Water Research Center, Institute of Northern Engineering, University of Alaska Fairbanks, 441 Duckering Building, P.O. Box 755860, Fairbanks, AK 99775-5860, USA. (matt.nolan@uaf.edu)

G. Liston, Colorado State University, CO, USA.

V. L. Sharpton, Geophysical Institute, University of Alaska Fairbanks, Fairbanks, AK 99775-5860, USA.